Impact of Smart Transformers in the Electrical Distribution Grid

Francisco G. Gonçalves
DEEC, Instituto Superior Técnico,
Universidade de Lisboa,
Lisboa, Portugal,
franciscogracagoncalves@tecnico.ulisboa.pt

Sónia F. Pinto
INESC-ID Lisboa
DEEC, Instituto Superior Técnico,
Universidade de Lisboa,
Lisboa, Portugal,
soniafp@tecnico.ulisboa.pt

José F. Silva
INESC-ID Lisboa
DEEC, Instituto Superior Técnico,
Universidade de Lisboa,
Lisboa, Portugal,
fernando.alves@tecnico.ulisboa.pt

Abstract—Nowadays, due to the growing importance of renewable energy resources, many technical and operational challenges are imposed on the electrical distribution grid. In addition, the current electrical distribution grid may also present some problems, such as: (i) unbalanced power flow, (ii) network overload, (iii) presence of voltage harmonics and (iv) frequency and voltage instability. Therefore, there are several power electronics equipment that try to mitigate or solve these problems.

This dissertation presents the Smart Transformer, a technology based on power electronics converters, which is not only capable of managing power flows, but also has the ability to manage communication flows. The Smart Transformer was implemented with a 3-stage conversion architecture, with a high-frequency transformer in each of the three phases and also with the use of filters and, current and voltage controllers.

For the implementation and simulation of the Smart Transformer in the electrical distribution grid, the simulation program used was Simulink of Matlab, where several simulation scenarios were carried out in order to test the technology under study.

The main conclusions of the study reveal that the Smart Transformer is capable of operating properly in the distribution grid. In fact, this dissertation proves that it is not only able to withstand disturbances in the medium voltage grid, but it can also be used in several geographical areas since it can be applied to low voltage grids with different operating frequencies.

Keywords: Smart Transformer, Power Electronics, Power Flow, Communication Flow, Electrical Distribution Grid

I. INTRODUCTION

Nowadays, due to the growing importance of renewable energy resources, the poor supply of charging stations for electric vehicles (EV) and the limitation of the information flow between sources and control centres being unidirectional, many technical and operational challenges arise in the electrical distribution grids, creating many limitations for new technologies to operate correctly, [1].

In addition, the current electrical distribution grid can also present some problems, such as: (i) unbalanced power flow, (ii) network overload, (iii) presence of voltage harmonics, (iv) frequency instability and (v) voltage instability.

Taking into account the technical and operational challenges of the distribution grid mentioned above, power electronics plays a very important role, as it creates a link between loads and sources in the distribution grid. Additionally, it is the power electronics equipment that try to mitigate or solve these problems, thus making the network more controllable and also improving the Quality of Electrical Energy (QEE) [2].

The target of analysis in this dissertation is the Smart Transformer (ST), which is based on electronic power converters, but is not yet on the market as it is under study. The ST is able to manage not only energy flows, but also communication flows, thus being able to solve the challenges of the current electrical distribution network system. However, ST will have to compete in terms of low price, high efficiency and high viability in order to enter the market.

Nevertheless, the applicability of a ST may be compromised by the temperature variations of semiconductors, as a result of the highly dynamic energy profiles and frequent contingencies, such as failures and fast variations of the current, which characterize the current distribution grid [3]. In order to overcome this limitation, the modular architecture in the ST is used to (i) enable the implementation of an active thermal control, in order to control the temperature variation of each semiconductor, and (ii) internally route the energy flows, so that the transformer does not cease to be operational if any of the semiconductors breaks down due to a failure, for example, a sudden increase in temperature [4].

Some advantages of ST are the possibility of having several DC connections available and the ability to mitigate harmonics at the same time, making it possible to supply different DC and AC loads with different frequencies [5]. In addition, the conventional and renewable power plants can be efficiently managed using ST, allowing intelligent loads to be commanded to switch on at a specific time taking into account the energy cost, maximizing the demand-response balance [6]. It should be noted that these and other advantages of the ST will be presented later.

In short, the advantages that ST offers make it an important component in the electrical distribution grid. For this reason, the ST was chosen as the target of analysis of this thesis because it is expected that this technology could be the key to the development of the distribution grid, potentiating the introduction of new technologies, such as smart grids.

To conclude the introduction, we intend with this dissertation to study the effects of the ST on the electrical distribution grid so that it is possible to overcome the failures presented above. Therefore, the main objectives of this dissertation are:

- To develop a simplified model of a ST;
- To design controllers for the ST;
- To simulate the AC grid with the ST.

II. Related Work

A. The origin of the Smart Transformer

In 1968, McMurray created the Solid-State Transformer (SST), which was based on power electronic semiconductors [7].

The true application of SST only appeared in the 90s, for application in traction systems, such as trains, in order to ensure that transformers were less bulky and less heavy. In fact, SST provided a reduction in volume and weight of around 20% to 50% and an increase in efficiency of around 93% to 96%. However, this transformer was never produced industrially because the marginal gain in terms of volume and weight was reduced with the increase in the operating frequency of the electrical distribution grid from 16.6 Hz to 50 Hz [8].

As shown in Fig. 1, the main problems found in the application of SST in the traction system are the fact that the hardware gains are only in terms of volume and weight [8].

However, the gains from using a SST in distribution systems are much greater than the gains in the traction system, as it facilitates intelligent functionalities. In fact, SST can replace the low frequency transformer, allowing connection between the medium voltage (MV) grid and the low voltage (LV) grid, as well as providing DC connectivity and network services on the MV and LV sides. In this case, unlike the traction system, whose most important requirements are weight and volume, the primary requirements for SST in the distribution system are efficiency and reliability, as shown in Fig. 1, as it is not tolerable that there is an interruption in the supply of Electrical Energy, nor if there are high losses [8].

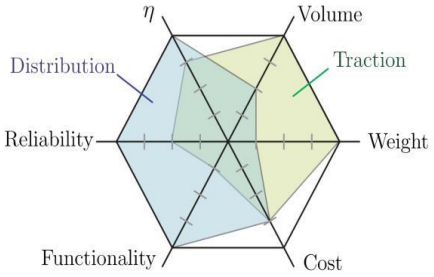

Fig. 1. Requirements for SST in traction and distribution systems [8]

In conclusion, the introduction of new features in the SST, namely control and communication, made this transformer intelligent, giving rise to the ST.

B. Flows of a Smart Transformer

The ST has the ability to communicate with the various local networks, and the information flow can be carried out in both directions, that is, both from the transformer to the network, and from the network to the transformer. For this reason, ST is a good option for mitigating or solving network problems.

The Fig. 2 shows the operating mode of the ST in the electrical distribution grid, showing the two types of flows that the ST is able to manage: in red the energy flow and in blue the communication flow. In addition to the flows, the several types of services that the ST can provide to the network are also observed, in which case services to industry, hospitals, smart homes, renewable energy systems, conventional power plants and energy storage systems.

C. Smart Transformer architecture

There are three types of architectures for the ST, which not only vary in the number of conversion stages, but also take into account the efficiency, reliability and additional functionalities of the ST.

The architectures, as well as their respective characteristics, are described below:

- One-stage architecture (MV-AC / LV-AC) and Two-stage architecture (MV-AC / MV-DC / LV-AC):
  - Reduced number of components;
  - Disturbances on one side of the ST can also affect the other side;
  - Does not allow the integration of DC networks on the LV side.
- Three-stage architecture (MV-AC / MV-DC / LV-DC / LV-AC):
  - DC connections on both sides;
  - It has more features, such as direct use of renewable DC sources;
  - Composed with a rectifier, an isolated DC-DC and an inverter.

To carry out the simulation, it will be used the three-stage conversion architecture because it is the only one that makes LV DC connectivity possible.

The next choice in terms of architecture is the degree of modularity and we can choose between a modular architecture and a non-modular architecture.

The modular architecture is based on the use of several low voltage/current modules, which are used as a single building block for the entire system. In addition to the high efficiency presented by this modularity [8], the voltage and power of the ST are easily scalable, which means that, if you want to increase these parameters, you just need to add more modules to the system. On the contrary, if you want to reduce the power, just disconnect enough modules until the desired value is reached. In addition to these features, the modular architecture also allows the implementation of maintenance and fault tolerance strategies or, in other words, the transformer can continue to work in case any of the blocks fails or breaks down. This is due to the fact that transformers are usually built with more modules than necessary for their correct functioning. Therefore, in case there is a failure of any of the modules, it is enough to change this block during the equipment maintenance, and until this change occurs, the transformer can continue to operate normally [8].

On the other hand, the non-modular architecture is based on a single structure that represents the system as a whole. The advantage of this type of modularity is the use of a smaller number of semiconductors, trigger circuits and sensors and the use of a single transformer. However, such features are not as advantageous as the features of modular architecture [8].

To sum up, due to the properties and benefits presented above, it is clear that the modular architecture is the option that brings the most advantages to the ST operation and, therefore, it should be chosen when you intend to implement a ST in the distribution grid.

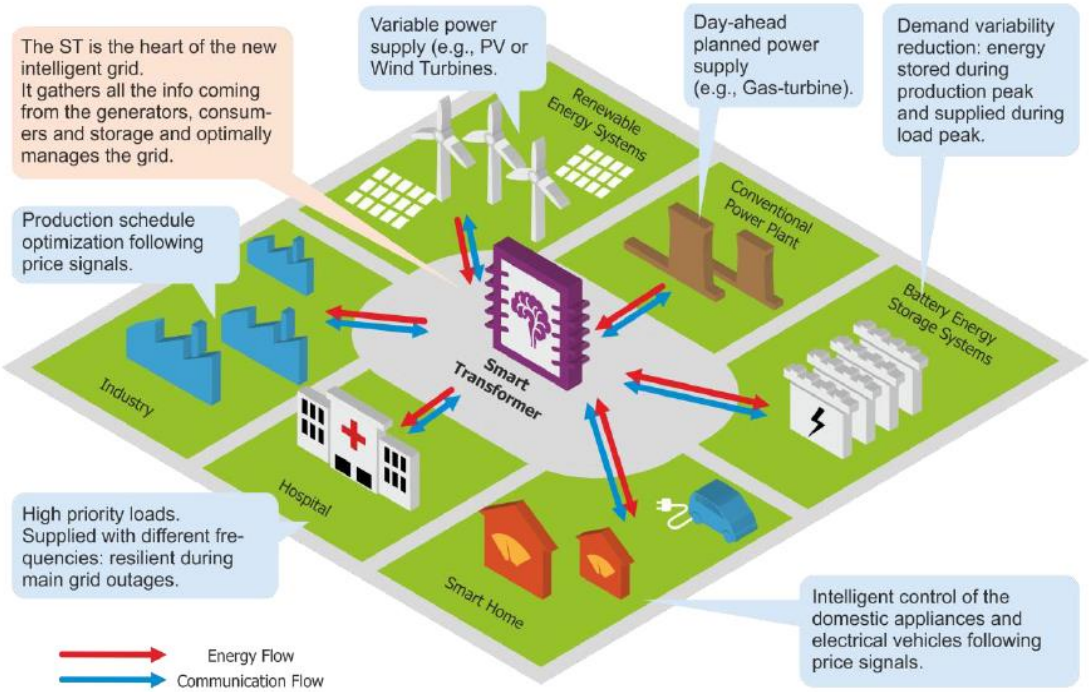

Fig. 2. The role of the Smart Transformer in the distribution grid [8]

D. Control Structure

The ST with a three-stage architecture can offer several services for MV DC and AC grids and also for LV DC and AC micro grids. In Fig. 3, we can see that the ST control structure can be divided into three levels:

- Layer 1, where are the network services that the ST can provide to the different grids;
- Layer 2, where are some basic control functionalities that allow the correct operation of the system;
- Layer 3, where is located the active thermal control, which allows controlling the temperature of the semiconductors depending on the operating conditions of the system. Therefore, it is possible to reduce the thermal stress of semiconductors that have their temperature too high, putting them on standby until their temperature is reduced. In this way, it becomes possible to avoid system failures due to high temperatures in semiconductors.

Then, in part A, layers 1 and 2 of the control structure will be analysed. Later, in part B, we will discuss the communication infrastructures, on which the ST system is dependent so that layers 1 and 2 can operate correctly.

Part A – *Ancillary Services*

From the possibility of DC connectivity, to the possibility of controlling voltages and frequencies in the MV and LV network, which enables a flexible and a robust distribution, there are several features that make the applicability of ST very interesting in the electrical distribution grid. Some of these functions are described below.

It is known that the ST has the ability to control the current absorbed from the MV grid, in order to satisfy the active power necessary for the load on the LV side, always taking into account the losses that occur during the process. Thus, one aspect to be taken into account is the fact that the transformer can vary the voltage to be converted from the MV grid in order to only transform the energy required for the LV grid, making the ST more flexible than currently used transformers. In addition, the ST can also control the voltage in the LV grid.

The reactive power represents a degree of freedom for the ST, which means the reactive power has the possibility of being individually controlled in each phase [9]. Additionally, reactive power can be decoupled between each terminal due to the presence of DC-links. With this feature, it is possible to obtain several functions, from working with a unitary power factor in the connection to the MV grid, to having harmonic compensation and voltage support on the MV side. Additionally, with its advanced controls, it can (i) support voltages in the MV network under critical conditions, injecting or absorbing reactive power, and (ii) solving problems in the LV grid, acting on each of the phases individually. It should be noted that, since the reactive power is isolated between each terminal, the LV side is prevented from absorbing the reactive power on the MV side and, consequently, it avoids matching the effects of the LV side on the MV side in direct voltage reduction.

In case there are high harmonics, the ST works as an active filter, reducing or eliminating the harmonics sent by the HV/MV transformer in the MV grid, and, consequently, manages to improve the energy quality in the MV distribution network.

Furthermore, regardless of the connected load, the ST is capable of generating three-phase sinusoidal and balanced voltages at the LV grid. The ST also has the ability to control the voltage and frequency of the LV grid and for that reason, it can interact with the voltage of loads and generators. For example, when a generator produces more energy than the LV grid consumes, the excess energy would be reverted to the MV

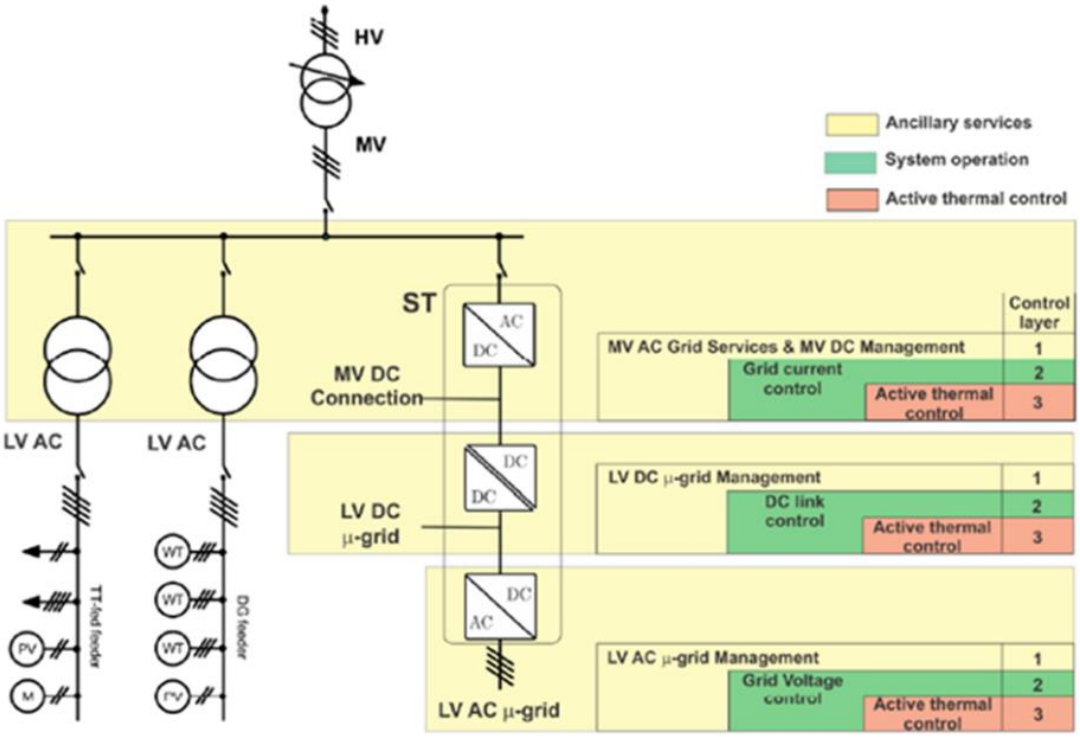

Fig. 3. Control and auxiliary services of the Smart Transformer [8].

grid, and consequently increasing the voltage of the MV grid. Using an ST, it is possible to interact with the generator, increasing the grid frequency [10] and, thus, decreasing the generator's energy production, avoiding the reverse energy flow to the MV grid.

Part B – *Communication Infrastructure*

A ST implemented in the electrical distribution grid behaves like a "brain", which not only manages and optimizes the energy flow of the network, but also regulates the information flow between the local network and the data centre.

The IEEE 2030 standard defines that there are three network hierarchies: (i) Private Networks, related to consumer properties; (ii) Wide Area Networks, related to the distribution domain; and (iii) the Core Networks, related to the generation and transmission of energy. In many applications, the ST is located in the distribution domain, facilitating the regulation of Wide Area Networks and the exchange of information between utilities and consumers [8].

The ST information flow in the distribution grid can be defined in three types:

- The first flow, between the different distribution systems;
- The second flow, between the ST and the local electrical systems;
- The third flow, between the ST and the information centres, or between two different ST, if there are multiple ST applied in the same network.

Most communication technologies used in smart grids can be applied when someone intends to use a ST in the distribution grid, and they will always depend on the communication architectures and control scenarios where they will be applied [11]. Furthermore, depending on the data rate and the distance, the communication technologies that can be used for Wide Area Networks are PLC, DSL, wireless mesh and cellular.

III. Methodologies

A. *Smart Transformer*

Due to the advantages mentioned in the literature review, it was decided to implement a three-stage conversion architecture to simulate the ST in the connection to the MV and LV grid.

The choice between three-phase or single-phase modules was conditioned by the advantages of each solution, as described below.

From a financial point of view, three-phase modules are economically more viable solutions in terms of acquisition and to assembly. However, in case of serious ST failures, the replacement or repair cost is higher, which makes single-phase machines more advantageous in future interventions.

In terms of dimensions and weight, single-phase modules are the best option and in case of installations in difficult-to-access locations, they may be the only way to make it possible to transport the equipment. However, three-phase machines take up less space in substations, a factor to be taken into account when the installation space is not large, for example, in cities.

Taking into account the relevant aspects of each solution and in order to guarantee low operating voltages and bidirectional power flow, the proposed ST (represented in Fig. 4) uses an association of 4 single-phase modules in each of the three phases, instead of using only a single three-phase converter on each conversion stage, avoiding this way a high DC voltage.

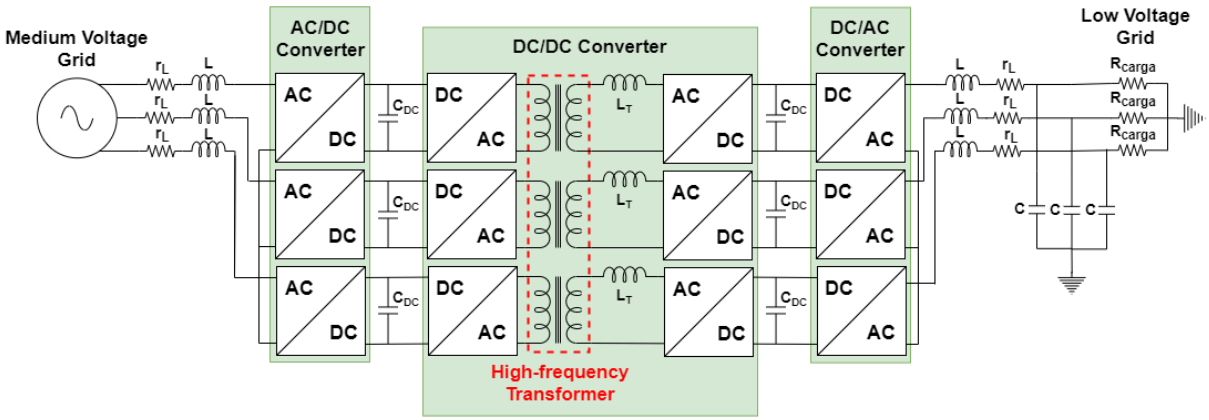

Fig. 4. Proposed scheme of the Smart Transformer

In Fig. 5. is represented the H-bridge topology, also called Full-bridge that was used to simulate each single-phase converter with high-frequency semiconductors. It is important to highlight that it was decided to use this topology because this converter can be operated as a rectifier (conversion from AC to DC) and as an inverter (conversion from DC to AC), allowing this way a bidirectional power flow.

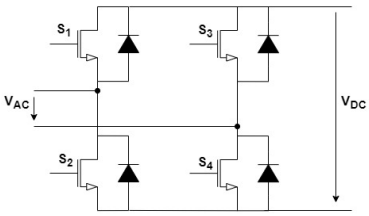

Fig. 5. H-bridge converter

To ensure galvanic isolation and a low volume of the ST, the DC/DC converter uses a high-frequency transformer in each phase. In Fig. 6 is possible to observe the Dual-Active-Bridge (DAB) topology used for the second conversion stage, where the high-frequency transformer connects the two H-bridge converters [12].

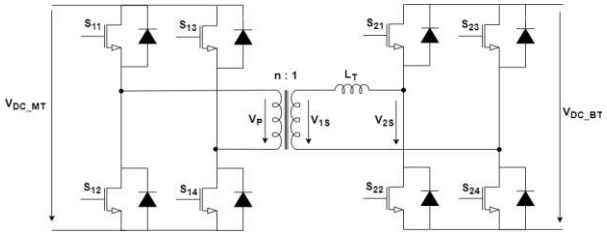

Fig. 6. DC/DC converter with DAB topology

The leakage reactance L_T of the transformer is given by

$$L_T = \frac{V_P.V_{2S}}{2\pi^2 n f_S P_0}\delta(\pi - \delta) \quad (1)$$

where δ is the phase shift angle between the tensions V_{1S} and V_{2S}, $P_0 = P/3$ is the monophasic power, being $P = 630\ kVA$ the total power of the ST, $f_s = 10\ kHz$ is the switching frequency and $n = V_P/V_{1S}$ is the number of windings in the high-frequency transformer [12].

B. AC Filter

The inductance L of the AC filter can be calculated using the following formula

$$L = \frac{U_{DC}.T_s}{2.(N_m - 1).\Delta i_L} \quad (2)$$

, where N_m is the number of levels of each converter ($N_m = 3$), U_{DC} is the DC voltage, $T_s = 1/f_s$ is the switching period and $\Delta i_L = 2\sqrt{3} \times THD_i \times i_{L_{RMS}}$ is the AC current ripple with $THD_i = 3\%$ [13].

Considering that the losses of the inductances of each phase represent 1% of the total power of each converter, r_L is given by (3) [14].

$$r_L = 0.01\frac{P_0}{{i_{L_{RMS}}}^2} \quad (3)$$

Since it was used a three-level pulse width modulation technique for the LV DC/AC converters, the value of capacitance C is

$$C = \frac{U_{DC}.{T_s}^2}{32.L.\Delta V_0} \quad (4)$$

, where it was imposed a maximum AC voltage (V_0) ripple of 2%, $\Delta V_0 = 0{,}02.V_0$ [13].

C. DC Filter

The DC filter is composed of only one capacitor, C_{DC}, connected in parallel between the three conversion stages. Therefore, each capacitance can be calculated by (5), where we know that $\omega = 2\pi f$ is the angular frequency with $f = 50\ Hz$ and it was imposed a maximum DC voltage ripple of 10%, $\Delta U_{DC} = 0{,}1.U_{DC}$ [13].

$$C_{DC} = \frac{P_0}{\omega.U_{DC}.\Delta U_{DC}} \quad (5)$$

D. AC Current Controller

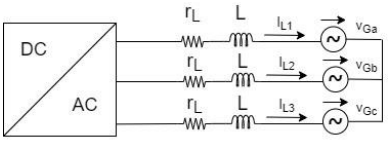

Fig. 7. DC/AC converter and its respective AC filter

To design the AC current controller, we started by writing the equations of the current dynamics, i_{L1}, i_{L2} and i_{L3}, in dq

coordinates using the Concordia and Park transformation. The value of i_{Ld} and i_{Lq} was synchronized with the value of the grid voltages, v_{Gd} and v_{Gq}. The dynamics of the currents are also dependent on the PWM input voltages, v_d and v_q, and on the coupling terms, ωi_{Lq} e ωi_{Ld} [14]. Thus, the equations of current dynamics written in canonical form can be observed in (6) [13].

$$\begin{cases} \frac{di_{Ld}}{dt} = \frac{v_d}{L} - \frac{r_L}{L} i_{Ld} + \omega i_{Lq} - \frac{v_{Gd}}{L} \\ \frac{di_{Lq}}{dt} = \frac{v_q}{L} - \frac{r_L}{L} i_{Lq} - \omega i_{Ld} - \frac{v_{Gq}}{L} \end{cases} \quad (6)$$

In order to ensure decoupling between the control actions d and q, the system of equations in (6) was linearized and two auxiliary variables were created, H_{id} and H_{iq}, as can be seen in equation (7) [13].

$$\begin{cases} \frac{di_{Ld}}{dt} = -\frac{r_L}{L} i_{Ld} + \frac{1}{L} H_{id} \\ \frac{di_{Lq}}{dt} = -\frac{r_L}{L} i_{Lq} + \frac{1}{L} H_{iq} \end{cases} , where \begin{cases} H_{id} = v_d + \omega i_{Lq} - v_{Gd} \\ H_{iq} = v_q - \omega i_{Ld} - v_{Gq} \end{cases} \quad (7)$$

Through the linearized equations in (7), it is possible to model the inverter as a first order transfer function, $G_{inv}(s)$, in which its differential gain, K_{di}, is unity and its delay, $T_{di} = T_s/2$ [13].

$$G_{inv}(s) = \frac{K_{di}}{1+sT_{di}} \leftrightarrow G_{inv}(s) = \frac{1}{1+sT_{di}} \quad (8)$$

Then, to guarantee a null static error [15], it was used a proportional integral compensator (PI), and its transfer function is given by the following equation [13].

$$G_{PI}(s) = \frac{sT_{zi}+1}{sT_{pi}} = \frac{sT_{zi}}{sT_{pi}} + \frac{1}{sT_{pi}} = K_{pi} + \frac{K_{ii}}{s} \quad (9)$$

To design the current controller it is necessary to obtain the closed-loop transfer function of the entire current control system. Therefore, taking into account that the zero of the PI compensator in (9) is coincident with the pole introduced by the grid filter, then

$$T_{zi} = \frac{L}{R_T} \quad (10)$$

, where R_T represents the equivalent grid resistance.

In Fig. 8 is presented the block diagram of the AC current controller, where α_i represents the gain of the current sensor.

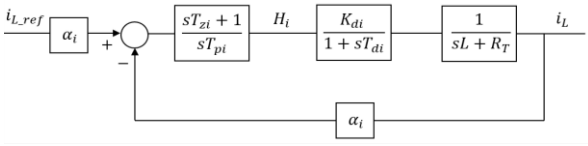

Fig. 8. Block diagram of the AC Current Controller

The closed-loop transfer function of Fig. 8 is [13]

$$\frac{i_L(s)}{i_{L\_ref}(s)} = \frac{\frac{\alpha_i K_{di}}{T_{di} T_{pi} R_T}}{s^2 + s\frac{1}{T_{di}} + \frac{\alpha_i K_{di}}{T_{di} T_{pi} R_T}} \quad (11)$$

Finally, comparing the denominator of (11) with the denominator of the second order transfer function written in canonical form in (12), it is possible to obtain the value of T_{pi}, considering a damping factor of $\xi = \sqrt{2}/2$ [13].

$$G_2(s) = \frac{{\omega_n}^2}{s^2 + 2\,\xi\omega_n . s + {\omega_n}^2} \quad (12)$$

$$T_{pi} = \frac{4.\xi^2.\alpha_i.T_{di}.K_{di}}{R_T} \leftrightarrow T_{pi} = \frac{2.\alpha_i.T_{di}}{R_T} \quad (13)$$

E. DC Voltage Controller

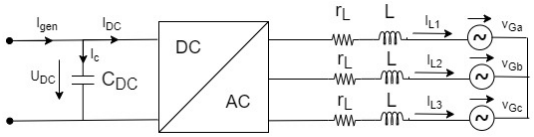

Fig. 9. DC/AC converter and its respective AC and DC filters

If we have the AC current controlled, the converter and its AC current controller can be represented by the following transfer function [13][16]

$$\frac{i_{DC}(s)}{i_{L\_ref}(s)} \approx \frac{G_i}{\alpha_i} \frac{1}{1+sT_{dv}} \quad (14)$$

, where $T_{dv} = 20\,ms$ and $G_i = V_{AC_{max}}/(2.U_{DC})$ is the gain of the AC current controller in each phase.

In Fig. 10, is represented the DC voltage controller block diagram, also using a PI compensator and where α_v represents the voltage sensor gain.

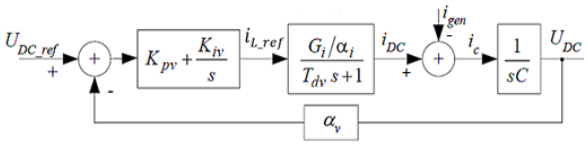

Fig. 10. Block diagram of the DC Voltage Controller

Equation (15) shows the closed-loop transfer function of the DC voltage controller shown in Fig. 10 [13].

$$\frac{U_{DC}}{U_{DC\_ref}} = \frac{\frac{\alpha_v G_i K_{pv} + sK_{iv}}{\alpha_i \quad T_{dv} C}}{s^3 + s^2\frac{1}{T_{dv}} + s\frac{\alpha_v G_i K_{pv}}{\alpha_i T_{dv} C} + \frac{\alpha_v G_i K_{iv}}{\alpha_i T_{dv} C}} \quad (15)$$

Comparing the denominator of the transfer function in (15) with the third degree polynomial written in canonical form in (16), we can obtain the proportional voltage gain, K_{pv} in (17), and the integral voltage gain, K_{iv} in (18), which constitute the PI block of the voltage controller [13].

$$P_3(s) = s^3 + 1.75\omega_0 s^2 + 2.15{\omega_0}^2 s + {\omega_n}^3 \quad (16)$$

$$K_{pv} = \frac{2.15 C \alpha_i}{1.75^2 \alpha_v G_i T_{dv}} \quad (17)$$

$$K_{iv} = \frac{C\alpha_i}{1.75^3 \alpha_v G_i {T_{dv}}^2} \quad (18)$$

F. AC Voltage Controller

The AC voltage in the MV grid is imposed on the ST and, therefore, cannot be controlled by the ST. As a result, the AC voltage controller can only be used to control the AC voltage of the LV grid.

The AC voltage controller is identical to the DC voltage controller shown above. The converter and its AC current controller are represented by the same transfer function

$$\frac{i_{DC}(s)}{i_{L\_ref}(s)} \approx \frac{G_i}{\alpha_i} \frac{1}{1+sT_{dv}} \tag{19}$$

however, $T_{dv} = T_s/2$ and $G_i = 1$ [17].

The block diagram of the AC voltage controller is the same as in Fig. 10 and the remaining expressions written in (15), (17) and (18) remain unchanged.

G. DC Current Controller

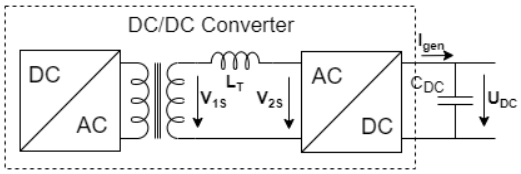

Fig. 11. DC/DC converter and DC filter on the LV side of ST

Through equation (1) it is possible to regulate the bidirectional power flow of the ST by controlling the phase shift angle, δ, between voltages V_{1S} and V_{2S}. If δ is positive, the energy transit is carried out from the MV side to the LV side. However, if negative, the energy transit is carried out in the opposite direction.

Using an integral compensator instead of a PI compensator, the block diagram of the DC current controller is shown in Fig. 12 [15].

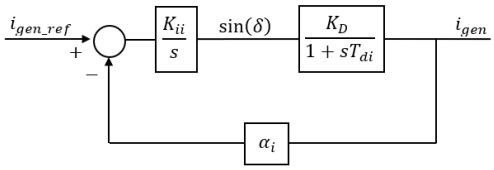

Fig. 12. Block diagram of the DC Current Controller

Equation (20) shows the differential gain of the DC current controller [15].

$$K_D = \frac{V_{1S}.V_{2S}}{2.\pi.f_S.L_T.U_{DC}} \tag{20}$$

The closed-loop transfer function, [15], of the DC current controller of Fig. 12 is

$$\frac{i_{gen}(s)}{i_{gen\_ref}(s)} = \frac{\frac{\alpha_i K_{ii} K_D}{T_{di}}}{s^2 + s\frac{1}{T_{di}} + \frac{\alpha_i K_{ii} K_D}{T_{di}}} \tag{21}$$

Comparing the denominator of (21) with the denominator of the second order transfer function written in canonical form in (12), it is possible to obtain the value of the integral gain, K_{ii}, considering a damping factor of $\xi = \sqrt{2}/2$ [15].

$$K_{ii} = \frac{1}{4.\xi^2.T_{di}.K_D.\alpha_i} \leftrightarrow K_{ii} = \frac{1}{2.T_{di}.K_D.\alpha_i} \tag{22}$$

IV. Results and Discussion

A. Scenario 1: Normal operating condition

In the first scenario, it was performed an analysis of the ST under normal operating conditions, without any disturbance in the MV and LV grids.

The main simulation parameters used in scenario 1 are found in table 1.

Table 1. Main Parameters of scenario 1

Parameters	Values
P_{ST} $(triphasic)$	630 kVA
P_{ST} $(monophasic)$	210 kVA
$f_{switching}$	10 kHz
V_{RMS_MV}	10 kV
f_{MV}	50 Hz
V_{RMS_LV}	400 V
f_{LV}	50 Hz
$P_{consumed}$ $(triphasic)$	594 kVA
$P_{consumed}$ $(monophasic)$	198 kVA
R_{load}	269,3602 $m\Omega$

The AC voltage is imposed by the MV grid and, therefore, the value observable in graph a) of Fig. 13 is presented in (23).

$$V_{AC\_MV_{max}} = \frac{10\,000}{\sqrt{3}} \times \sqrt{2} = 8\,165\ V \tag{23}$$

The AC current controllers of the MV grid are designed to limit the AC current value between the maximum current value calculated in (24) and its negative value. Looking at graph b) of Fig. 13, the controller is operating correctly as the measured value is less than $I_{AC\_MV_{max}}$. In addition, the controller errors are close to zero, which means that the controller is managing to stabilize the AC current at the desired set point.

$$I_{AC\_MV_{max}} = \frac{210\,000}{\frac{10\,000}{\sqrt{3}}} \times \sqrt{2} = 51{,}44\ A \tag{24}$$

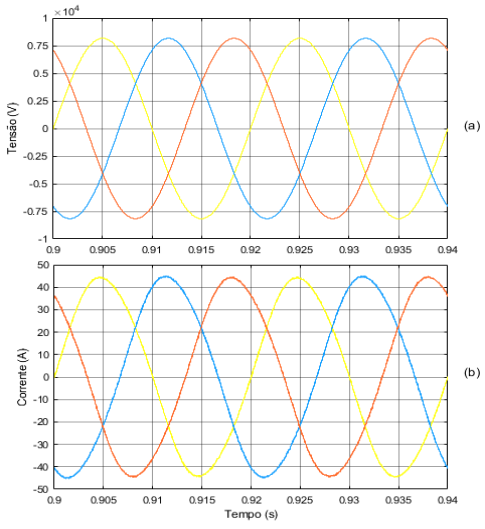

Fig. 13. a) AC voltage in the MV grid; b) AC current in the MV grid

In Fig. 14, it is possible to observe the DC voltage of the DC filters capacitances for the MV side. For these DC voltage controllers, the reference value chosen was $V_{DC\_MV_{ref}} = 10\,000\ V$ and, as it can be seen, the controllers are correctly

stabilizing the DC voltage and are also having an error close to zero.

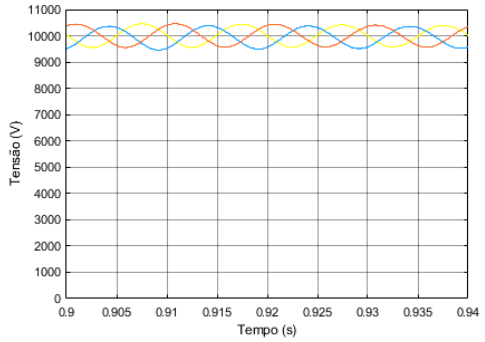

Fig. 14. Voltage at the DC filters capacitors on the MV side

For the DC voltage controllers on the LV side, the reference value chosen was $V_{DC\_LV_{ref}} = 400\ V$. Analysing Fig. 15, the controllers are correctly controlling the DC voltage on the LV side and also have an error close to zero.

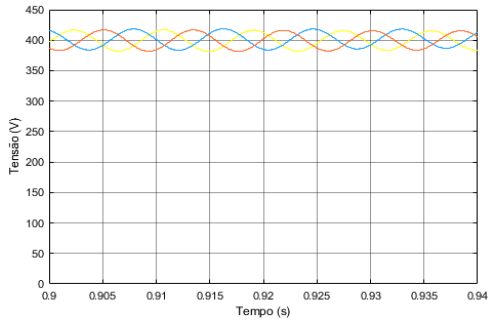

Fig. 15. Voltage at the DC filters capacitors on the LV side

Fig. 16 shows the DC currents measured at the output of the DC/DC conversion stage at the LV side. The errors of the DC current controllers were close to zero, which demonstrates the correct control of the DC current. Even so, it is possible to calculate the expected value of the DC current in (25) and analysing the graph in Fig. 16, it can be seen that the measured value is similar to the calculated in (25).

$$P_{DC} = P_{consumed} \leftrightarrow I_{DC} = \frac{198\,000}{400} = 495\ A \qquad (25)$$

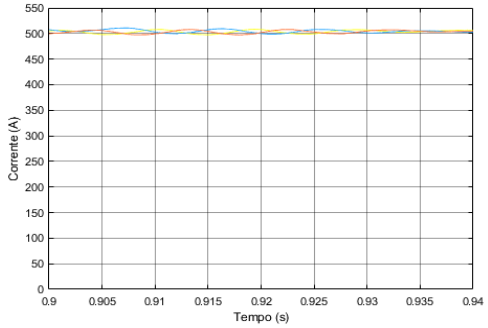

Fig. 16. DC current at the output of the DC/DC conversion stage

The AC voltage of the LV grid is controlled by an AC voltage controller that imposes as a reference value the maximum AC voltage calculated in (26) and, as it can be seen in graph a) of Fig. 17, the AC voltage controller is operating correctly.

$$V_{AC\_LV_{max}} = \frac{400}{\sqrt{3}} \times \sqrt{2} = 326{,}6\ V \qquad (26)$$

The AC current controllers of the LV grid are designed to limit the AC current value between the maximum value calculated in (27). Looking at graph b) of Fig. 17, the controller is operating correctly as the measured value is less than $I_{AC\_LV_{max}}$.

$$I_{AC\_LV_{max}} = \frac{210\,000}{\frac{400}{\sqrt{3}}} \times \sqrt{2} = 1\,286\ A \qquad (27)$$

Nevertheless, it is possible to calculate the expected value of the AC current in (28) and analysing the graph b) in Fig. 17, it can be seen that the measured value is similar to the calculated in (28).

$$P_{AC} = P_{consumed} \leftrightarrow I_{AC} = \frac{198\,000}{230} = 1\,217\ A \qquad (28)$$

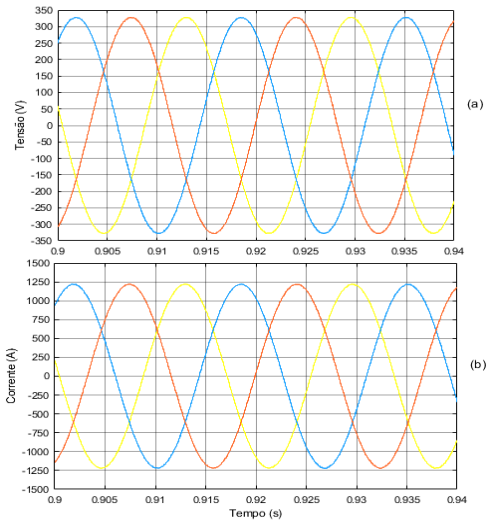

Fig. 17. a) AC voltage in the LV grid; b) AC current in the LV grid

B. *Scenario 2: Presence of voltage dips in the MV grid*

In the second scenario, it was performed an analysis of the behavior of the ST when faced with a situation of voltage dips (depth of 20% and duration of 40 *ms*) in the MV grid, which can be caused by the occurrence of defects or the connection of high power loads [18].

According to the standard EN 50160:2010 and the Quality of Service Regulation, a voltage dip is a "sudden decrease in the supply voltage to a value between 90% and 5% of the nominal voltage, followed by the re-establishment of voltage after a short time span. By convention, a voltage dip lasts from ten milliseconds to one minute." [19].

In graph a) of Fig. 18, it is possible to observe that the voltage dip caused a reduction in the input voltage from 8 165 *V* to 6 532 *V* during two periods. After the 0.84 seconds, the AC voltage returns to its original value of 8 165 *V*.

On the other hand, it can be analysed through graph b) of Fig. 18 that, during the presence of the voltage dip in the MV network, the AC current increased by approximately 10 *A*. After the dip dissipated, the network took about 80 *ms* to stabilize, this is, to return to its original value. During the entire process, the errors of the AC current controllers remained close to zero, which means that the AC current is

able to remain controlled even with the presence of voltage dips in the MV grid.

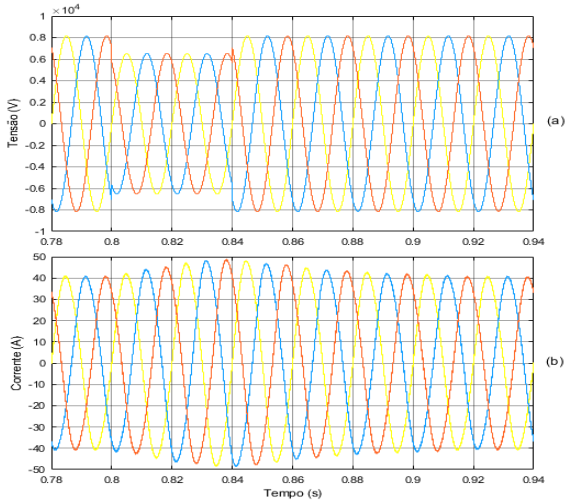

Fig. 18. a) AC voltage and b) AC current in the MV grid (scenario 2)

From Fig. 19, it is possible to conclude, as expected, that the AC voltage and AC current at the load terminals did not change, which proves the good behaviour of the ST against this type of disturbance. Both controllers had their errors close to zero, which confirms their correct operation.

The AC current value is smaller than the value presented for scenario 1 in (28) because the consumed power in this scenario was 180 kVA in each phase.

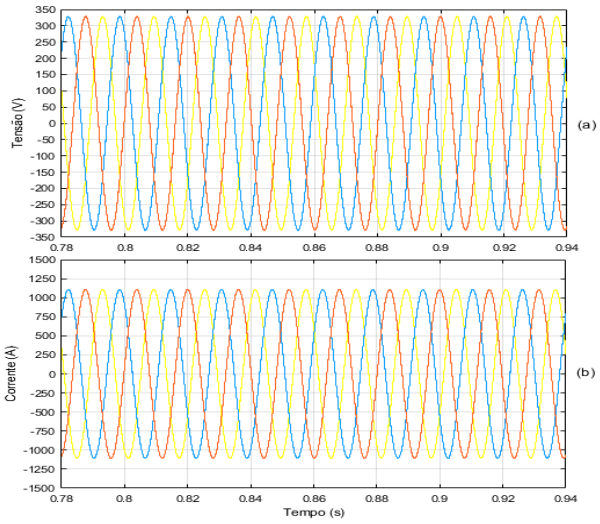

Fig. 19. a) AC voltage and b) AC current in the LV grid (scenario 2)

C. *Scenario 3:Presence of overvoltages in the MV grid*

In the third scenario, the ST was subjected to an overvoltage (depth of 10% and duration of 40 ms) in the MV grid that could be caused by atmospheric or electrostatic discharges.

According to the Electric Power Quality manual, transient overvoltage correspond to extremely fast variations in the voltage value, with durations between microseconds and seconds, and can reach very high peak values [20].

According to the standard EN 50160:2010, overvoltage are characterized by a temporary increase in the RMS value equal to 110% of the reference value [19].

In graph a) of Fig. 20 is possible to observe an overvoltage that caused a slight increase in the AC input voltage from 8 165 V to 8 982 V during two periods. After the overvoltage disappears at 0.84 seconds, the AC voltage returns to its original value of 8 165 V.

In graph b) of Fig. 20, it can be analyzed that during the presence of disturbance, the AC current decreased and it took about 60 ms to stabilize, after the overvoltage disappear. During the entire process, the errors of the AC current controllers remained close to zero, which means that the AC current is able to remain controlled.

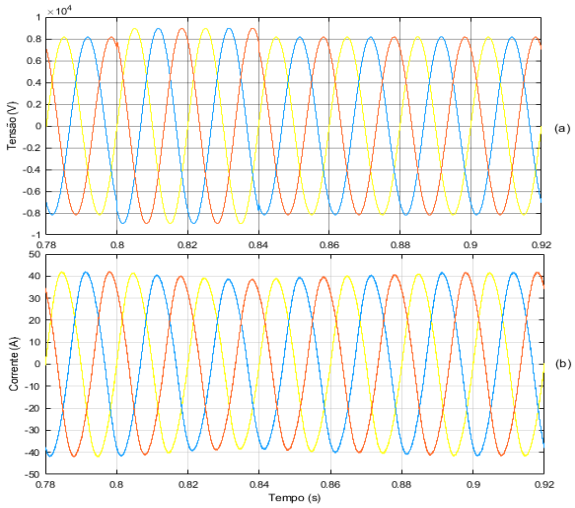

Fig. 20. a) AC voltage and b) AC current in the MV grid (scenario 3)

Given an overvoltage situation at the input side of ST, it is possible to see in Fig. 21 that the AC voltage and AC current at the load terminals did not suffer major changes, which shows the good response of the ST to this type of disturbance. Both controllers had their errors close to zero, which also supports their correct operation.

The AC current value is different from the value of the two previous scenarios because the consumed power in this scenario was 185 kVA.

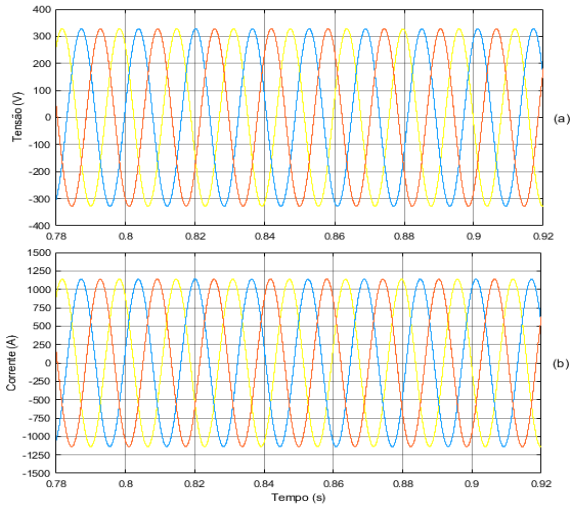

Fig. 21. a) AC voltage and b) AC current in the LV grid (scenario 3)

V. Conclusion

This dissertation aimed to study the impact of the ST on the electrical distribution grid, in order to try to overcome the technical and operational challenges of the distribution

system, as well as to be able to respond to the gaps imposed by traditional transformers.

It was developed a transformer with a 3-stage conversion architecture, using an association of four single-phase modules and a high-frequency transformer in each of the three phases of the ST. In addition to DC and AC filters, DC and AC current and voltage controllers were also created to control the currents and voltages of the entire system under analysis.

In the first instance, it was analysed the behaviour of the ST under normal operating conditions of the LV and MV grids. For this scenario, several load levels were studied, and it was possible to verify that all the controllers, as well as all the other components that constitute the ST, were able to operate correctly. However, it was verified that the ST was only able to supply 594 kV to the LV grid load, instead of the dimensioned value of 630 kV, thus constituting a limitation to the simulation.

However, the network does not always behave in an ideal way, being subject to several disturbances, and in this thesis two common disturbances were analysed. Therefore, the ST was subjected to sudden voltage variations, in the MV grid, in short periods of time (a 20% voltage dip and an overvoltage of 10%, both during two periods of the network), having behaved as expected in both scenarios. So, it was concluded that the ST was able to withstand sudden voltage variations in the MV grid and always maintaining the quality of service of the supply of sinusoidal and balanced three-phase voltages and currents to the LV grid.

The ST was also simulated with a LV grid with an operating frequency of 60 Hz. The only change that took place was a reduction in the period of the LV network, with all controllers continuing to operate correctly. To conclude, this ST has a wide geographic coverage as it can be applied in Europe, as it behaves well with an operating frequency of 50 Hz (as seen in scenario 1), as well as in some countries of South America, as it behaved well in the face of a 60 Hz LV grid, since this value is characteristic of some countries on this continent.

Finally, it was demonstrated that the ST has the ability to decouple the reactive power from its terminals because, when imposed by the simulation, it was able to absorb reactive power in the MV network without causing interference in the LV network, keeping the entire system working correctly.

In conclusion, all controllers designed for the ST functioned properly when submitted to both the normal and adverse scenarios, always presenting a good capacity of regulation. Furthermore, the waveforms of voltages and currents presented were practically sinusoidal without appreciable distortions, with only being visible a small oscillation from the semiconductors switching.

VI. Future Work

After completing this dissertation, new ideas emerged with a view to improve the proposed ST system, namely:

- Simulate the ST with more possible scenarios, both in the MV grid and in the LV grid, in order to test the ST operation when subjected to another type of disturbance, such as the presence of harmonics in the MV network;
- Understand what led to the limitation of the ST supplied power of 594 kV, instead of the dimensioned value of 630 kV to the LV network load, trying to solve this same problem in order to eliminate the limitation detected in Simulink;
- Restructure the converter, using a larger number of modules in series in each of the ST conversion stages, as it would allow simulating a system closer to reality;
- Implement a reactive power controller for the MV grid, in order to allow control of the reactive power that is absorbed or injected in the MV grid for the ancillary services of the ST in the distribution system.

Finally, the execution of the proposed ST would be an asset, as it would allow testing the equipment with real situations, which would enhance the development of this technology.

References

[1] E. J. Coster, J. M. A. Myrzik, B. Kruimer e W. L. Kling, "Integration Issues of Distributed Generation in Distribution Grids," *Proceedings of the IEEE,* vol. 99, nº 1, pp. 28 - 39, Janeiro 2011.

[2] M. Liserre, T. Sauter e J. Y. Hung, "Integrating Renewable Energy Sources into the Smart Power Grid," *IEEE Industrial Electronics Magazine,* vol. 4, nº 1, pp. 18 - 37, Março 2010.

[3] H. Wang, M. Liserre e F. Blaabjerg, "Toward Reliable Power Electronics: Challenges, Design Tools, and Opportunities," *IEEE Industrial Electronics Magazine,* vol. 7, nº 2, pp. 17 - 26, Junho 2013.

[4] M. A. e M. Liserre, "Impact of active thermal management on power electronics design," *Microelectronics Reliability,* vol. 54, nº 9 - 10, pp. 1935 - 1939, Setembro-Outubro 2014.

[5] S. Brüske, G. De Carne e M. Liserre, "Multi-frequency power transfer in a smart transformer based distribution grid," em *IECON 2014 - 40th Annual Conference of the IEEE Industrial Electronics Society*, Dallas, TX, USA, 29 Outubro - 1 Novembro 2014.

[6] B. Olek e M. Wierzbowski, "Local Energy Balancing and Ancillary Services in Low-Voltage Networks with Distributed Generation, Energy Storage, and Active Loads," *IEEE Transactions on Industrial Electronics,* vol. 62, nº 4, pp. 2499 - 2508, Abril 2015.

[7] W. Mcmurray, "Power converter circuits having a high frequency link". Patente US3517300, 1968.

[8] M. Liserre, G. Buticchi, M. Andresen, G. De Carne, L. F. Costa e Z.-X. Zou, "The Smart Transformer: Impact on the Electric Grid and Technology Challenges," IEEE Industrial Electronics Magazine, vol. 10, nº 2, pp. 46 - 58, Junho 2016.

[9] G. De Carne, G. Buticchi, M. Liserre, C. Yoon e F. Blaabjerg, "Voltage and current balancing in Low and Medium Voltage grid by means of Smart Transformer," em 2015 IEEE Power & Energy Society General Meeting, Denver, CO, USA, 26-30 Julho 2015.

[10] G. De Carne, G. Buticchi, M. Liserre e C. Vournas, "Frequency-Based Overload Control of Smart Transformers," em 2015 IEEE Eindhoven PowerTech, Eindhoven, Netherlands, 29 Junho - 2 Julho 2015.

[11] V. C. Gungor, D. Sahin, T. Kocak, S. Ergut, C. Buccella, C. Cecati e G. P. Hancke, "Smart Grid Technologies: Communication Technologies and Standards," IEEE Transactions on Industrial Informatics, vol. 7, nº 4, pp. 529 - 539, Novembro 2011.

[12] G. M. Paraíso, S. F. Pinto e J. F. Silva, "Modelling and nonlinear control of Dual-Active Bridge converters for DC microgrids," em *IECON 2019 - 45th Annual Conference of the IEEE Industrial Electronics Society*, Lisboa, Portugal, 2019.

[13] F. Silva, S. Pinto e J. Santana, Conversores Comutados para Energias Renováveis, 2016/2017.

[14] R. A. Alexandre, S. F. Pinto e J. J. Santana, "Energy storage system for grid connection and island operation," em *2016 IEEE International Smart Cities Conference (ISC2)*, Trento, Italy, 12-15 Sept. 2016.

[15] R. G. Gago, S. F. Pinto e J. F. Silva, "G2V and V2G electric vehicle charger for smart grids," em *2016 IEEE International Smart Cities Conference (ISC2)*, Trento, Italy, 12-15 Sept. 2016.

[16] S. Pinto, J. F. Silva, F. Silva e P. Frade, Design of a Virtual Lab to Evaluate and Mitigate Power Quality Problems Introduced by Microgeneration, 2011.

[17] P. Fernandes, *Transformador Electrónico de Potência para Aplicações em Sistemas de Energia,* Tese de Mestrado, IST, 2014.

[18] D. Faria e H. Jorge, *Qualidade de Energia Eléctrica – Caracterização de Cavas de Tensão em Redes MT,* 2013.

[19] P. E. Networks, *EN 50160 - Voltage characteristics of electricity supplied,* 2010.

[20] C. Patrao, J. Delgado e A. Almeida, *Manual de Qualidade da Energia Eléctrica,* Portuguese National Utility - EDP Distribuição, Dezembro.